Article:
Chen, J, Liu, R orcid.org/0000-0003-0627-3184, Ngoduy, D orcid.org/0000-0002-0446-5636 et al. (1 more author) (2016) A new multi-anticipative car-following model with consideration of the desired following distance. Nonlinear Dynamics, 85 (4). pp. 2705-2717. ISSN 0924-090X

https://doi.org/10.1007/s11071-016-2856-4

Noname manuscript No.
(will be inserted by the editor)

A new multi-anticipative car-following model with consideration of the desired following distance

Jianzhong Chen · Ronghui Liu · Dong Ngoduy · Zhongke Shi

Received: date / Accepted: date

Abstract We propose in this paper an extension of the multi-anticipative optimal velocity car-following model to consider explicitly the desired following distance. The model on the following vehicle's acceleration is formulated as a linear function of the optimal velocity and the desired distance, with reaction-time delay in elements. The linear stability condition of the model is derived. The results demonstrate that the stability of traffic flow is improved by introducing the desired following distance, increasing the time gap in the desired following distance or decreasing the reaction-time delay. The simulation results show that by taking into account the desired following distance as well as the optimal velocity, the multi-anticipative model allows longer reaction-time delay in achieving stable traffic flows.

Keywords Multi-anticipative model · Desired following distance · Stability analysis · Traffic flow

1 Introduction

Car-following models, which mimic the behaviour of individual vehicles and drivers, have been widely studied. Researchers have developed different types of car-following models such as stimulus-response models, safe-distance models, desired headway models, psychophysical models and artificial intelligence

J. Chen
College of Automation, Northwestern Polytechnical University, Xi'an 710072, China
Institute for Transport Studies, University of Leeds, Leeds LS2 9JT, UK
E-mail: jzhchen@nwpu.edu.cn

R. Liu · D. Ngoduy
Institute for Transport Studies, University of Leeds, Leeds LS2 9JT, UK

Z. Shi
College of Automation, Northwestern Polytechnical University, Xi'an 710072, China

models (see reviews in Refs. [1-3]). Among them, the stimulus-response models assume that the actions taken by the considered vehicle's driver mainly depend on the stimulus received from the preceding vehicles. The stimulus may include the velocity of the considered vehicle, the headway, the velocity difference between the considered vehicle and its leading vehicle, etc. [4,5].

The Gazis-Herman-Rothery (GHR) model [6], first introduced by Chandler et al. [7], is a well-known stimulus-response model. The model was later extended and calibrated by many researchers [1,2]. In this type of models, the acceleration/deceleration of the considered vehicle depends on the velocity of the vehicle, the headway, and the velocity difference between the considered vehicle and its leader. Helly [8] introduced the desired following distance factor and added some terms into the original GHR model. The resulting model is a linear model.

The optimal velocity (OV) model first developed by Bando et al. [9] is another well studied stimulus-response model. In the OV model, the difference between the optimal velocity and the velocity of the considered vehicle is assumed to be the stimulus for the driver's actions. The OV model is capable of reproducing many observed traffic phenomena, such as the evolution of traffic congestion and the stop-and-go traffic. However, the calibration using field data suggests that the OV model produces unrealistically high acceleration and deceleration [10,11]. Helbing and Tilch [10], and Jiang et al. [11] introduced the velocity difference into the OV model, and proposed the generalized force model and the full velocity difference (FVD) model, respectively. The authors in [12-15] extended the FVD model to consider the varying road condition, the inter-vehicle communication and the anticipation driving behavior.

With the development and application of the intelligent transportation systems, drivers can get the information of multiple vehicles ahead. The multi-anticipative car-following models have been gradually developed. In the multi-anticipative situation, the stimulus can be multiple headways, multiple velocity differences, etc. There are mainly two types of approaches to model the multi-anticipative behaviour.

The first type of multi-anticipative models involves the distance or the velocity difference between two adjacent vehicles. Nagatani [16] and Ge et al. [17] extended the difference equation model [18] by taking into account the next-nearest-neighbour interaction and an arbitrary number of vehicles ahead, respectively. The OV model was generalized and extended to include multiple look-ahead (many-neighbour interaction) by Wilson et al. [19]. The results presented by the authors confirm the necessity of multiple look-ahead considerations. Chen et al. [20] incorporated the drivers' reaction delay into the multi-anticipative model [19]. They found that the multi-anticipative consideration could partially compensate the unfavourable effect induced by driver reaction delays. Yu et al. [21] suggested an extended OV model by taking into account the headways of arbitrary number of preceding vehicles and the relative velocity. They derived the stability condition and the modified Korteweg-de Vries (KdV) equation near the critical point to describe the traffic behaviours. Li and Liu [22] proposed an extended FVD model by introducing the relative

velocities of arbitrary number of vehicles ahead. Jin et al. [23] introduced the headway and the velocity difference of two preceding vehicles into the FVD model, and derived the KdV and modified KdV equations to describe the traffic behaviours. The models developed by Xie et al. [24], and Peng and Sun [25] incorporated both headways and relative velocities of multiple preceding vehicles into the FVD model. Ngoduy [26] investigated the linear stability of the multi-anticipative OV model and intelligent driver model [27] with delays. Li et al. [28] put forwards a multi-anticipative model, which considered multiple headway, velocity and acceleration difference.

In the second type of multi-anticipative models, the headway or the velocity difference involved is the difference between the considered vehicle and an arbitrary preceding vehicle. Lenz et al. [29] extended the OV model by taking into account multi-vehicle interactions. They found that the multi-anticipative consideration can improve the stability of traffic flow. The extended model can reproduce the fundamental properties of traffic flow and the synchronized flow. Treiber et al. [30] proposed the multi-anticipative intelligent driver model and compared which with the standard intelligent driver model [27]. The results indicate that the multi-anticipation is a basic aspect of human driving behaviour. The authors [31,32] extended the Helly model [8] to incorporate multiple vehicle interactions. They performed an empirical study of multi-anticipation, and concluded that the multi-anticipation was indeed present. Farhi et al. [33] presented a multi-anticipative piecewise-linear model [34]. Hu et al. [35] introduced the driver reaction delays and multi-velocity-difference into the model [29], and suggested an extended multi-anticipative delay model. They found that introducing the velocity difference information of multiple vehicles ahead improves the stabilization of traffic flow.

However, none of the above multi-anticipative OV models considered the effect of the desired following distance. In real traffic, the drivers would attempt to achieve not only a desired or an optimal velocity, but also a desired following distance. They would adjust their acceleration/deceleration according to this distance and this optimal velocity.

In this paper, we extend the OV model [29] by an explicit consideration of the desired following distance and propose a new extended multi-anticipative car-following model. A long wavelength linear stability analysis is conducted and the stability condition is derived. Finally, numerical simulations are carried out to demonstrate the theoretical results.

The following notations are used in this paper:

Index

n	index of vehicle
t	time instant (s)
m	number of preceding vehicles considered

Model variables

$x_n(t)$	position of vehicle n at time t (m)
$\Delta x_{n+j,n}(t)$	headway $x_{n+j}(t) - x_n(t)$ (m) between the vehicle n and the leading vehicle $n+j$

$v_n(t)$	velocity of vehicle n at time t (m/s)
$\Delta x_n^{des}(t)$	desired following distance (m)
Model parameters	
α	sensitivity coefficient of a driver to the difference between the optimal velocities and the actual velocity (1/s)
β	sensitivity coefficient of a driver to the distance ($1/s^2$)
t_d	reaction-time delay of drivers (s)
p_j	weight of the optimal velocity function
q_j	weight of the distance $\Delta x_{n+j,n}(t-t_d)/j$
s_0	stopping distance, including vehicle length (m)
T	time gap (s)
a and b	step-function parameters for modelling β
s_c	critical distance (m) in the step-function of β
V_1 and V_2	parameters of the optimal velocity function (m/s)
C_1	parameter of the optimal velocity function (m^{-1})
C_2	parameter of the optimal velocity function
L_c	average length of vehicles (m)

2 Model

Lenz et al. [29] proposed an extended OV model to take into account multi-vehicle interactions. The resulting multi-anticipative model was generalised by Wilson et al. [19] as:

$$\frac{\mathrm{d}^2 x_n(t)}{\mathrm{d}t^2} = \alpha \left[\sum_{j=1}^{m} p_j V\left(\frac{\triangle x_{n+j,n}(t)}{j} \right) - \frac{\mathrm{d}x_n(t)}{\mathrm{d}t} \right], \tag{1}$$

where $V(\cdot)$ is the optimal velocity function, and the weight $p_j > 0$ and $\sum_{j=1}^{m} p_j = 1$.

Hu et al. [35] introduced the reaction-time delay of drivers into the model (1). Eq. (2) shows the multi-anticipative model with the time delay.

$$\frac{\mathrm{d}^2 x_n(t)}{\mathrm{d}t^2} = \alpha \left[\sum_{j=1}^{m} p_j V\left(\frac{\triangle x_{n+j,n}(t-t_d)}{j} \right) - \frac{\mathrm{d}x_n(t)}{\mathrm{d}t} \right]. \tag{2}$$

In their original formulation, Hu et al. [35] also included a term to represent the effect of the relative velocity.

The above multi-anticipative models consider only an optimal following velocity. In real traffic situations, drivers also attempt to achieve a desired distance from vehicles ahead. This factor is shown to have an important influence on traffic flow [8,36,37]. In this paper, we extend the models (1) and (2) by

capturing explicitly the effect of the desired following distance, as well as that of the optimal velocity and the time delay. Our new model is formulated as:

$$\begin{aligned}\frac{\mathrm{d}^2x_n(t)}{\mathrm{d}t^2} = \alpha &\left[\sum_{j=1}^{m} p_j V\left(\frac{\triangle x_{n+j,n}(t-t_d)}{j}\right) - \frac{\mathrm{d}x_n(t)}{\mathrm{d}t}\right] \\ &+ \beta\left[\sum_{j=1}^{m} q_j\left(\frac{\triangle x_{n+j,n}(t-t_d)}{j}\right) - \Delta x_n^{des}(t)\right],\end{aligned} \tag{3}$$

where the weight $q_j > 0$ and $\sum_{j=1}^{m} q_j = 1$. In contrast to the models (1) and (2), our proposed model (3) indicates that a driver adjusts his acceleration/deceleration not only according to the optimal velocity, but also according to the desired following distance. When $\beta = 0$ and $t_d = 0$, the model (3) is reduced to the model described by Eq. (1). It is worth noting that the relative velocity and the desired distance were also considered in a multi-anticipative version of the Helly model [31,32]. In this model, the acceleration of the nth vehicle is determined by the weighted velocity difference between the current vehicle and the vehicles in front, and a weighted sum of the difference between the actual and the desired distance headway to the $n+j$ vehicle in front. While in our model (3) the nth vehicle tends to achieve both the optimal velocity and the desired distance, the acceleration is determined according to the difference between the optimal velocity given by a weighted sum of several OV functions and the velocity of vehicle n, and the difference between a weighted sum of the distance (same as that in OV function) and the desired following distance to the vehicle $n+1$.

In models (2) and (3), it is assumed that a driver can sense his velocity instantaneously and only the argument of the headway $\Delta x_{n+j,n}$ contains the delay time, which is similar to the delayed car-following models [20,26,38-41]. The case that the headway, the velocity and the velocity difference are all evaluated at the delayed time is mainly discussed in the autonomous cruise control literatures [42,43]. For other traffic flow models with time delay, we refer to [44-49].

In the literatures, the desired following distance $\Delta x_n^{des}(t)$ has been modelled as a linear function of the vehicle velocity $v_n(t)$ [8], and other more complex forms [8,27,50]. However, the studies of Helly [8] and Van Winsum [51] revealed that the desired following distance can be reasonably determined based on the linear form. In this paper, we adopt the linear form:

$$\Delta x_n^{des}(t) = s_0 + T v_n(t), \tag{4}$$

where the time gap T describes the dependence of the desired following distance on the velocity.

Following [52], we take the step function for β as :

$$\beta = \begin{cases} a, & h \le s_c, \\ b, & h > s_c, \end{cases} \tag{5}$$

where $h = \sum_{j=1}^{m} q_j \left(\frac{\triangle x_{n+j,n}(t-t_d)}{j} \right)$. Eq. (5) represents a two-step effect of the desired following distance has different effects in different distance h.

In model (3), the weights p_j and q_j reflect the effect of the leading vehicle $n+j$ on the vehicle j. It is reasonable to assume that this effect gradually reduces with increasing j, i.e. $p_{j+1} < p_j$ and $q_{j+1} < q_j$. For convenience, we assume $p_j = q_j$ and select p_j following [25]:

$$\sum_{j=1}^{m} p_j = 1, \quad p_j = \begin{cases} (l-1)/l^j, \text{ for } j \neq m, \\ 1/l^{j-1}, \quad \text{for } j = m, \end{cases} \tag{6}$$

where the constant l can be taken as $l = 2, 3, \cdots$. Eq. (6) gives a decreasing function of p_j with increasing j value. This is to represent a decreasing influence as the leading vehicle is furthering ahead. In our simulations, l is arbitrarily chosen as 6, thus for a $m = 2$, we have $p_1 = 5/6$ and $p_2 = 1/6$ which gives the weight on the influence of the immediate leading vehicle at 5/6, while that of the second vehicle ahead at 1/6. Following [10], the OV function is chosen as:

$$V(\triangle x) = V_1 + V_2 \tanh[C_1(\Delta x - L_c) - C_2], \tag{7}$$

where $V_1 = 6.75$ m/s, $V_2 = 7.91$ m/s, $C_1 = 0.13$ m^{-1} and $C_2 = 1.57$. In Eq. (7), the average length of vehicles L_c is taken as 5 m in our simulations.

3 Linear stability analysis

Stability is an important property of any car-following model. Chow [53] first performed an analytical analysis of the stability conditions of the GHR model [6]. Liu and Li [54] analysed the stability of the multi-regime car-following model [5] through a numerical analysis. In this section, we investigate the long wavelength linear stability of the new model (3) and derive analytically the linear stability condition.

For convenience, the RHS of Eq. (3) is abbreviated as function $f(\Delta x_{n+1,n}, \cdots, \Delta x_{n+m,n}, v_n)$. In the uniform traffic flow, all vehicles move with the constant headway s_e. According to the work of Wilson and Ward [55], a set of stability conditions can be analysed if there is a function v_e, such that $f(s_e, \cdots, ms_e, v_e(s_e)) = 0$.

In our model, there exists such $v_e(s)$ and it has the form

$$v_e(s) = \frac{\alpha V(s) + \beta(s - s_0)}{\alpha + \beta T}. \tag{8}$$

Then, the uniformly steady-state solution for Eq. (3) is given by

$$x_n^{(0)}(t) = s_e n + v_e(s_e)t. \tag{9}$$

Let $y_n(t)$ denotes the small deviation from the steady-state solution $x_n^{(0)}(t)$: $x_n(t) = x_n^{(0)}(t)+y_n(t)$. Substituting it into Eq. (3) and linearizing the resulting equation, one can obtain

$$\frac{\mathrm{d}^2 y_n(t)}{\mathrm{d}t^2} = \alpha \left[\sum_{j=1}^{m} \frac{1}{j} p_j V'(s_e) \triangle y_{n+j,n}(t-t_d) \right] - (\alpha+\beta T) \frac{\mathrm{d}y_n(t)}{\mathrm{d}t} + \beta \left[\sum_{j=1}^{m} \frac{1}{j} q_j \triangle y_{n+j,n}(t-t_d) \right], \tag{10}$$

where $\triangle y_{n+j,n}(t-t_d) = y_{n+j}(t-t_d) - y_n(t-t_d)$ and $V'(s_e) = \mathrm{d}V(\triangle x_n)/\mathrm{d}\triangle x_n \mid_{\triangle x_n = s_e}$.

Expanding $y_n(t) = A\exp(ikn + zt)$, we obtain the following equation of z:

$$z^2 + (\alpha+\beta T)z - \alpha V'(s_e)\mathrm{e}^{-zt_d} \sum_{j=1}^{m} \frac{p_j}{j}(\mathrm{e}^{ikj}-1) - \beta \mathrm{e}^{-zt_d} \sum_{j=1}^{m} \frac{q_j}{j}(\mathrm{e}^{ikj}-1) = 0. \tag{11}$$

By expanding $z = z_1(ik) + z_2(ik)^2 + \cdots$ and inserting it into Eq. (11), we obtain the first- and second-order terms of ik:

$$z_1 = \frac{\alpha V'(s_e) + \beta}{\alpha + \beta T}. \tag{12}$$

$$z_2 = \frac{-z_1^2 + \alpha \sum_{j=1}^{m} p_j V'(s_e)(\frac{j}{2} - t_d z_1) + \beta \sum_{j=1}^{m} q_j (\frac{j}{2} - t_d z_1)}{\alpha + \beta T}. \tag{13}$$

For long wavelength modes, the uniformly steady-state flow is stable if $z_2 > 0$, while the uniformly flow becomes unstable when $z_2 < 0$. Thus, the neutral stability condition is

$$\alpha = \frac{-c_2 - \sqrt{c_2^2 - 4c_1c_3}}{2c_1}, \tag{14}$$

where

$$c_1 = \left(V' t_d - \sum_{j=1}^{m} \frac{j}{2} p_j \right), c_2 = \left(V' + \beta T V' t_d + \beta t_d - 2\beta T \sum_{j=1}^{m} \frac{j}{2} p_j \right),$$

$$c_3 = \left(\beta - \beta^2 T^2 \sum_{j=1}^{m} \frac{j}{2} p_j \right).$$

For small disturbance of long wavelength, the uniform traffic flow becomes unstable provided that

$$\alpha < \frac{-c_2 - \sqrt{c_2^2 - 4c_1c_3}}{2c_1}. \tag{15}$$

Fig. 1 shows the neutral stability lines in the space (s_e, α) for different values of a in the step function (5). The another parameter b in (5) is taken as 0. The

parameter values are set as: $t_d = 0.2$ s, $T = 1.8$ s, $m = 3$ and $s_c = 70$ m. In Fig. 1, the apex of each line corresponds to the critical point. The area below each line is the unstable region, in which the density waves appear. While above each line, the traffic flow is stable and traffic jams do not occur. From Fig. 1, we can see that the stable region increases with increasing value of a. Note that the case of $a = 0$ in the step function (5) corresponds to the model (2) when $b = 0$. Hence, the result indicates that by considering the desired following distance, the traffic flow becomes more stable.

Fig. 2 illustrates the neutral stability curves for different values of the time gap T in Eq. (4). The parameters are $m = 2$, $t_d = 0.2$ s and $a = 0.5$ s^{-2}. For comparison, the result of the model (2) is also depicted in Fig. 2. We can see that the critical point obtained from the model (3) is lower than that of the model (2). The stable region of our new model (3) increases with the increase of T. This shows that the stability of traffic flow is improved by increasing the time gap in the desired following distance.

Fig. 3 shows the neutral stability curves for different values of m when $a = 0.3$ s^{-2}. The other parameter values used are the same as those in Fig. 1. It is found that the critical points and the neutral stability lines decrease with the increase of m, which means that the stability of traffic flow is strengthened by the multi-anticipative consideration. The curves for the cases of $m = 3$ and $m = 5$ are almost coincided. This indicates that considering three vehicles ahead is enough, which is similar to the results of other studies [17,20,25].

The neutral stability curves for different values of t_d are shown in Fig. 4. The parameter is set as $a = 0.3$ s^{-2}. The other parameter values used are the same as those in Fig. 1. From Fig. 4, it can be seen that the neutral stability curves are lowered with the decrease of t_d. This means that the traffic flow will be more stable when the reaction-time delay of drivers decreases.

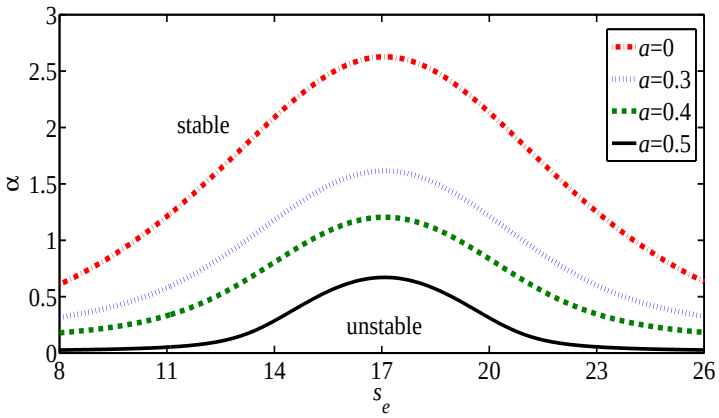

Fig. 1 Phase diagram in the space (s_e, α) for different values of a

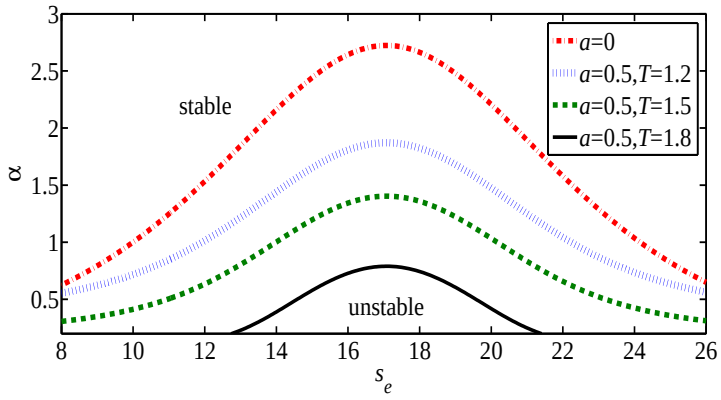

Fig. 2 Phase diagram in the space (s_e, α) for different values of a and T

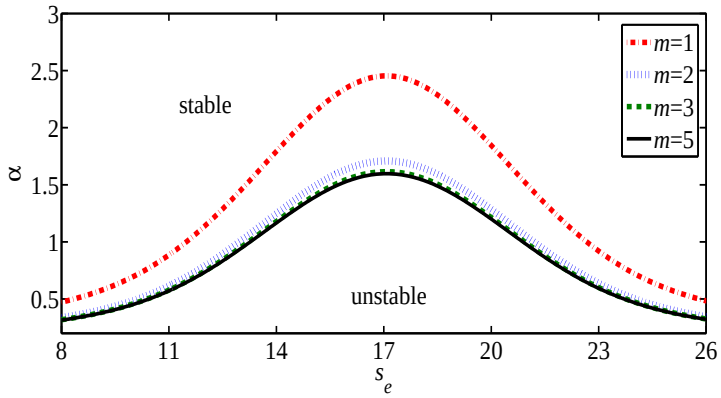

Fig. 3 Phase diagram in the space (s_e, α) for different values of m

4 Numerical simulations

We perform numerical simulations for our proposed new model (3) under periodic boundary condition. We adopt the following numerical integration scheme [12,13,56] for Eq. (3):

$$\begin{aligned} v_n(t+\Delta t) &= v_n(t) + \frac{\mathrm{d}v_n(t)}{\mathrm{d}t}\Delta t, \\ x_n(t+\Delta t) &= x_n(t) + v_n(t)\Delta t + \frac{1}{2}\frac{\mathrm{d}v_n(t)}{\mathrm{d}t}(\Delta t)^2, \end{aligned} \tag{16}$$

where $v_n(t+\Delta t)$ and $x_n(t+\Delta t)$ are the velocity and position of vehicle n at time t, respectively. In our simulations, the time step Δt is set to 0.01 s.

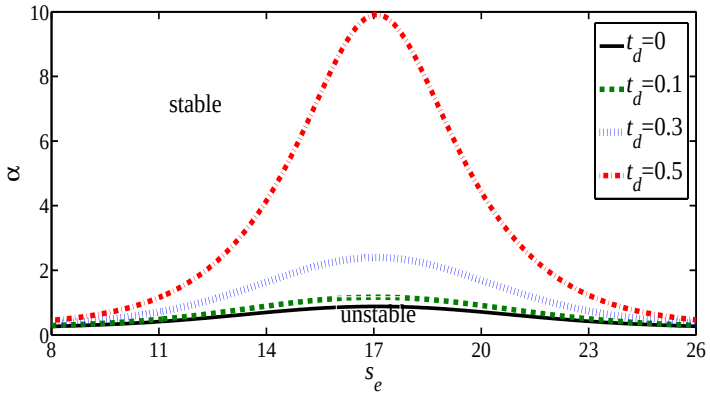

Fig. 4 Phase diagram in the space (s_e, α) for different values of t_d

We consider $N = 100$ vehicles running on a single-lane circular road of length $L = 1500$ m. The initial disturbance is set as that in [11]:

$$x_1(0) = 1 \text{ m}, \ x_n(0) = (n-1)L/N \text{ m}, \ \text{for } n \neq 1, \tag{17}$$

$$\dot{x}_n(0) = V(L/N) \text{ m/s}. \tag{18}$$

In the following simulation, the distance h in the step-function (5) does not exceed $s_c = 70$ m, thus we adopt constant β instead of the step-function (5).

4.1 Stabilization effect of the desired following distance

We investigate the effect of the desired following distance on the stability of traffic flow in this subsection. Fig. 5 shows the space-time evolution of the headway for different values of β at time t between 1000 s and 1200 s. The parameters are set as $t_d = 0.2$ s, $T = 1.8$ s and $m = 3$. Here after, the sensitivity α and the stopping distance s_0 are set and remain constant at 1.25 s^{-1} and 7.4 m, respectively. When $\beta = 0$, the result corresponds to that of the model (2). When $\beta = 0$, 0.1, 0.2 and 0.3 s^{-2}, the homogeneous flow evolves into congestion as time develops. This congestion corresponds to stop-and-go traffic. In addition, the amplitude of headway variation decreases with the increase of β. This indicates that the introduction of the desired following distance can improve the stability of traffic flow.

The effect of the desired following distance can be further illustrated in Fig. 6, where the snapshot of velocities of all vehicles at $t = 300$ s and $t = 1000$ s are shown. When $\beta = 0$, the negative velocity appears, which is unrealistic and needs to be overcome. It is found that from Fig. 6 the negative velocity is avoided by introducing the desired following distance.

In the congested flow, the motion of vehicles forms a hysteresis loop in the headway-velocity phase space. Fig. 7 exhibits the hysteresis loops for $\beta = 0$,

0.2, 0.3 and 0.4 s^{-2}. From Fig. 7, we can see that the size of the hysteresis loop decreases with the increase of β, which means that the amplitude of velocity variation is smaller and the traffic flow is more stable. When $\beta = 0.4$ s^{-2}, the instability condition (15) is not satisfied, and the traffic flow is stable. We can see that the hysteresis loop will degenerate to a point.

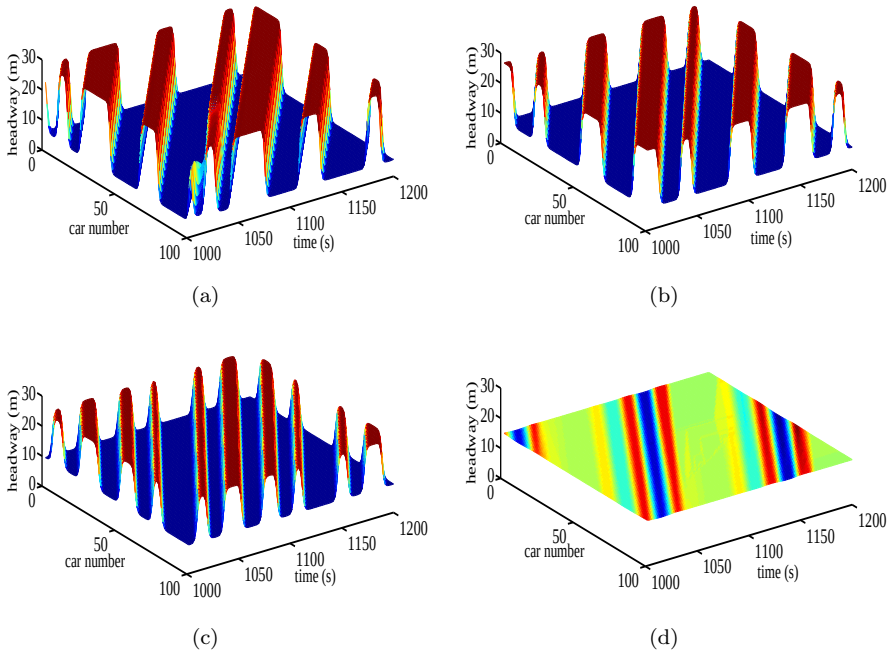

Fig. 5 Space-time evolution of the headway for different values of β. (a) $\beta = 0$, (b) $\beta = 0.1$, (c) $\beta = 0.2$, (d) $\beta = 0.3$

4.2 Effect of the time gap

In this subsection, we choose $m = 2$ to explore the impact of the time gap T in the desired following distance. Fig. 8 exhibits the space-time evolution of the headway for different values of T at time t from 1000 s to 1200 s. The parameters are set as $t_d = 0.2$ s and $\beta = 0.25$ s^{-2}. We can find that the amplitude of headway decreases as the time gap increases, which indicates that the stability of traffic flow is strengthened.

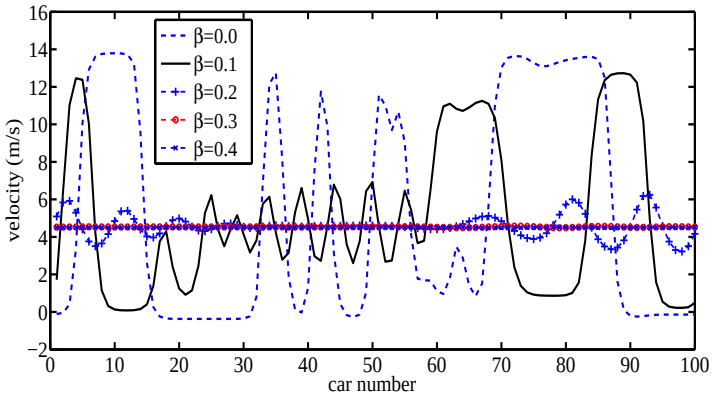

(a)

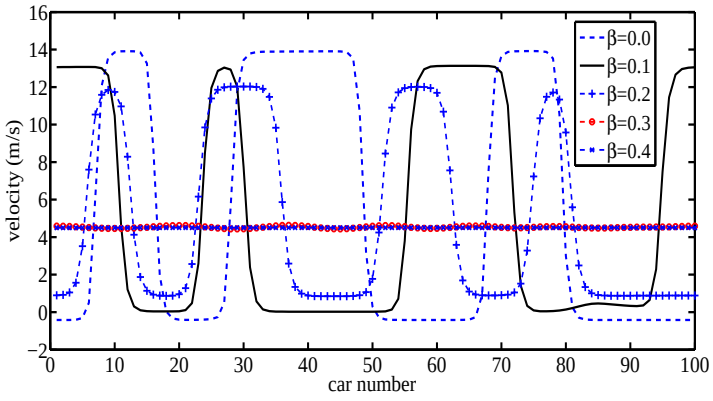

(b)

Fig. 6 Snapshot of velocities of all vehicles for different values of β. (a) $t = 300$ s, (b) $t = 1000$ s

4.3 Effect of the reaction-time delay

We study in this subsection the effect of different reaction time delays of drivers on traffic flow. Fig. 9 illustrates the snapshot of velocities of all vehicles for $t_d = 0.25$ s, 0.35 s and 0.45 s when $t = 2000$ s. The parameter is $T = 1.8$ s. When $m = 3$ and $\beta = 0$ (see Fig. 9(a)), the result is same as that of the model (2). The unrealistic negative velocity appears, which indicates the model does not allow these delay times. From Fig. 9(b), we can see that for the same parameters the multi-anticipative model (3) with $\beta = 0.5$ s^{-2} avoids the negative velocity and allows larger delay times. This suggests that introducing the desired following distance is more reasonable and realistic. The result of $m = 1$ and $\beta = 0.5$ s^{-2} is shown in Fig. 9(c). Comparing Fig. 9(b) with Fig. 9(c), we find that when $t_d = 0.35$ s, the negative velocity occurs for the case of

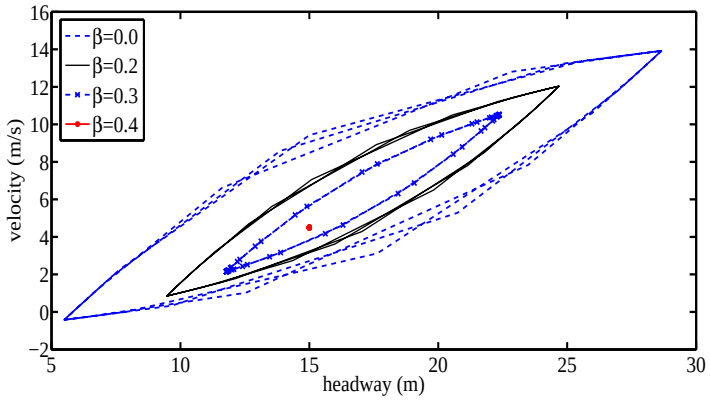

Fig. 7 The hysteresis loops for $\beta = 0$, 0.2, 0.3 and 0.4 s^{-2}

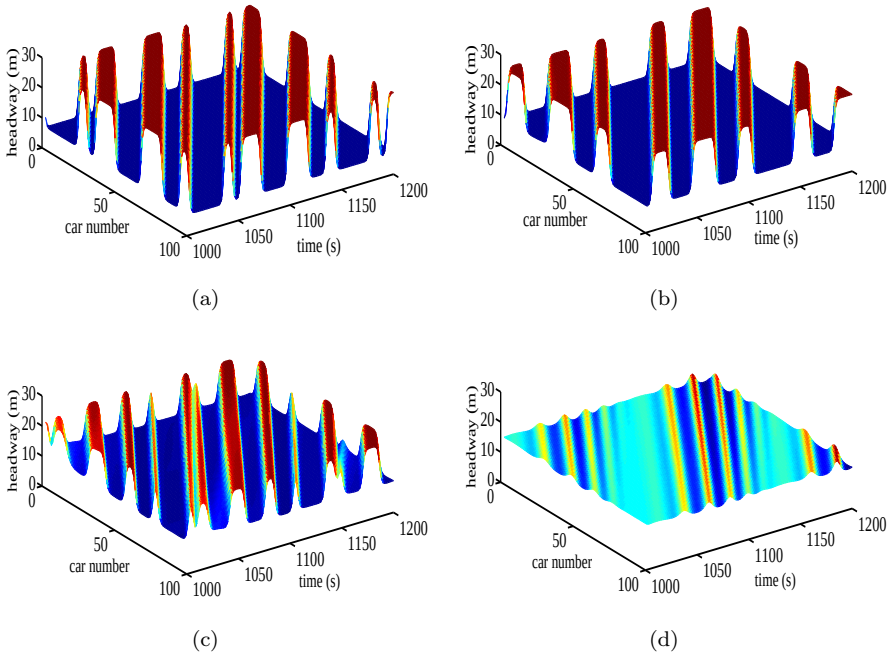

Fig. 8 Space-time evolution of the headway for different values of T. (a) $T = 1.2$, (b) $T = 1.5$, (c) $T = 1.8$, (d) $T = 2.0$

$m = 1$, while this deficiency is overcome for the case of $m = 3$. This indicates that multi-anticipative consideration allows larger delay times. In addition, we can also see from Fig. 9 that the amplitude of the curves decreases with decreasing t_d, which means that the stability of traffic flow can be enhanced with the decrease of the reaction-time delay.

4.4 Effect of the multi-anticipation

In this subsection, we explore the effect of considering different number of preceding vehicles. Fig. 10 shows the snapshot of velocities of all vehicles for $m = 1$, 2 and 3 when $t = 3500$ s. The parameters are set as $t_d = 0.2$ s, $T = 1.8$ s and $\beta = 0.3$ s^{-2}. We can see from Fig. 10 that the amplitude of velocity variation decreases with the increase of m. This means that multi-anticipative consideration can improve the stability of traffic flow. Fig. 11 illustrates the hysteresis loops for different values of m. From Fig. 11, we find that the hysteresis loop is reduced with increasing of m, which further shows that the multi-anticipation has an important effect on the stability of traffic flow.

5 Conclusions

In this paper, we presented an extended multi-anticipative model with explicit consideration of the effect of the desired following distance on the following vehicle's acceleration and deceleration. The model is formulated as a linear combination of the optimal velocity and desired following distance. The reaction-time delay of drivers is incorporated in the effect of the distance headway. A linear stability analysis is carried out and the stability condition is obtained. The simulation results demonstrate that by introducing the desired following distance, not only can the stabilization of traffic flow be enhanced, but the deficiency of unrealistic negative velocity can also be avoided. This confirms that the desired following distance has an important influence on traffic behaviour and is an important factor to be considered in car-following models. The analytical and numerical results show that increasing the time gap in the desired following distance can also enhance the stability of traffic flow. Although the stability of traffic flow is weakened with the increase of the reaction-time delay of drivers, it is essential and is necessary to construct realistic traffic flow models. We found that the model considering multi-anticipative behaviour and the desired following distance allow larger reaction-time delay in producing stable traffic flows.

It must be pointed out that we adopt the linear function to model the desired following distance in this study. There are other methods of depicting the desired following distance, such as the nonlinear functions. Thus, we should investigate the performance of them, and compared them with the linear form in our future work. Furthermore, the model parameters will be calibrated by using observation data. In addition, the model will be extended to derive the multi-anticipative macroscopic traffic flow model based on the transformation method between the microscopic variables and the macroscopic ones.

Acknowledgements This work was supported by the National Natural Science Foundation of China (Grant No. 11102165), the Natural Science Basis Research Plan in Shaanxi Province of China (Grant No. 2015JM1013), the Fundamental Research Funds for the Central Universities (Grant No. 3102015ZY050), and the UK Rail Safety and Standards Board

(Grant No. T1071). The first author would like to acknowledge the China Scholarship Council for sponsoring his visit to the University of Leeds.

References

1. Brackstone, M., McDonald, M.: Car-following: a historical review. Transp. Res. F **2**, 181-196 (1999)
2. Aghabayk, K., Sarvi, M., Young, W.: A state-of-the-art review of car-following models with particular considerations of heavy vehicles. Transp. Rev. **35**, 82-105 (2015)
3. Bonsall, P., Liu, R., Young, W.: Modelling safety-related driving behaviour-impact of parameter values. Transp. Res. A **39**, 425-444 (2005)
4. Chowdhury, D., Santen, L., Schadschneider, A.: Statistical physics of vehicular traffic and some related systems. Phys. Rep. **329**, 199-329 (2000)
5. Wang, J., Liu, R., Montgomery, F.O.: A car following model for motorway traffic. Transp. Res. Rec. **1934**, 33-42 (2005)
6. Gazis, D.C., Herman, R., Rothery, R.W.: Nonlinear follow-the-leader models of traffic flow. Oper. Res. **9**, 545-567 (1961)
7. Chandler, R.E., Herman, R., Montroll, E.W.: Traffic dynamics: studies in car following. Oper. Res. **6**, 165-184 (1958)
8. Helly, W.: Simulation of bottlenecks in single lane traffic flow. In: Proceedings of the symposium on theory of traffic flow, pp. 207-238 (1959)
9. Bando, M., Hasebe, K., Nakayama, A., Shibata, A., Sugiyama, Y.: Dynamics model of traffic congestion and numerical simulation. Phys. Rev. E **51**, 1035-1042 (1995)
10. Helbing, D., Tilch, B.: Generalized force model of traffic dynamics. Phys. Rev. E **58**, 133-138 (1998)
11. Jiang, R., Wu, Q.S., Zhu, Z.J.: Full velocity difference model for a car-following theory. Phys. Rev. E **64**, 017101 (2001)
12. Tang, T.Q., Wang, Y.P., Yang, X.B., Wu, Y.H.: A new car-following model accounting for varying road condition. Nonlinear Dyn. **70**, 1397-1405 (2012)
13. Tang, T.Q., Shi, W.F., Shang, H.Y., Wang, Y.P.: A new car-following model with consideration of inter-vehicle communication. Nonlinear Dyn. **76**, 2017-2023 (2014)
14. Zheng, L.J., Tian, C., Sun, D.H., Liu, W.N.: A new car-following model with consideration of anticipation driving behavior. Nonlinear Dyn. **70**, 1205-1211 (2012)
15. Kang, Y.R., Sun, D.H., Yang, S.H.: A new car-following model considering driver's individual anticipation behavior. Nonlinear Dyn. **82**, 1293-1302 (2015)
16. Nagatani, T.: Stabilization and enhancement of traffic flow by the next-nearest-neighbor interaction. Phys. Rev. E **60**, 6395-6401 (1999)
17. Ge, H.X., Dai, S.Q., Dong, L.Y., Xue, Y.: Stabilization effect of traffic flow in an extended car-following model based on an intelligent transportation system application. Phys. Rev. E **70**, 066134 (2004)
18. Nagatani, T., Nakanishi, K., Emmerich, H.: Phase transition in a difference equation model of traffic flow. J. Phys. A **31**, 5431-5438 (1998)
19. Wilson, R.E., Berg, P., Hooper, S., Lunt, G.: Many-neighbour interaction and non-locality in traffic models. Eur. Phys. J. B **39**, 397-408 (2004)
20. Chen, J.Z., Shi, Z.K., Hu, Y.M.: Stabilization analysis of a multiple look-ahead model with driver reaction delays. Int. J. Mod. Phys. C **23**, 1250048 (2012)
21. Yu, L., Shi, Z.K., Zhou, B.C.: Kink-antikink density wave of an extended car-following model in a cooperative driving system. Commun. Nonlinear Sci. Numer. Simul. **13**, 2167-2176 (2008)
22. Li, Z.P., Liu, Y.C.: Analysis of stability and density waves of traffic flow model in an ITS environment. Eur. Phys. J. B **53**, 367-374 (2006)
23. Jin, Y.F., Xu, M., Gao, Z.Y.: KDV and Kink-antikink solitons in an extended car-following model. J. Comput. Nonlinear Dyn. **6**, 011018 (2011)

24. Xie, D.F., Gao, Z.Y., Zhao, X.M.: Stabilization of traffic flow based on the multiple information of preceding cars. Comm. Comp. Phys. **3**, 899-912 (2008)
25. Peng, G.H., Sun, D.H.: A dynamical model of car-following with the consideration of themultiple information of preceding cars. Phys. Lett. A **374**, 1694-1698 (2010)
26. Ngoduy, D.: Linear stability of a generalized multi-anticipative car following model with time delays. Commun. Nonlinear Sci. Numer. Simul. **22**, 420-426 (2015)
27. Treiber, M., Hennecke, A., Helbing, D.: Congested traffic states in empirical observations and microscopic simulations. Phys. Rev. E **62**, 1805-1824 (2000)
28. Li, Y.F., Sun, D.H., Liu, W.N., Zhang, M., Zhao, M., Liao, X.Y., Tang, L.: Modeling and simulation for microscopic traffic flow based on multiple headway, velocity and acceleration difference. Nonlinear Dyn. **66**, 15-28 (2011)
29. Lenz, H., Wagner, C.K., Sollacher, R.: Multi-anticipative car-following model. Eur. Phys. J. B **7**, 331-335 (1999)
30. Treiber, M., Kesting, A., Helbing, D.: Delays, inaccuracies and anticipation in microscopic traffic models. Physica A **360**, 71-88 (2006)
31. Ossen, S., Hoogendoorn, S.P.: Multi-anticipation and heterogeneity in car-following: empirics and a first exploration of their implications. In: IEEE Intelligent Transportation Systems Conference, pp. 1615-1620 (2006)
32. Hoogendoorn, S., Ossen, S., Schreuder, M.: Empirics of multi-anticipative car-following behavior. Transp. Res. Rec. **1965**, 112-120 (2006)
33. Farhi, N., Haj-Salem, H., Lebacque, J.P.: Multi-anticipative piecewise-linear car-following model. Transp. Res. Rec. **2315**, 100-109 (2012)
34. Farhi, N.: Piecewise linear car-following modeling. Transp. Res. C **25**, 100-112 (2012)
35. Hu, Y.M., Ma, T.S., Chen, J.Z.: An extended multi-anticipative delay model of traffic flow. Commun. Nonlinear Sci. Numer. Simul. **19**, 3128-3135 (2014)
36. Treiber, M., Kesting, A.: Traffic flow dynamics: data, models and simulation. Springer, Germany (2013)
37. Addison, P.S., Low, D.J.: A novel nonlinear car-following model. Chaos **8**, 791-799 (1998)
38. Davis, L.C.: Modifications of the optimal velocity traffic model to include delay due to driver reaction time. Physica A **319**, 557-567 (2003)
39. Orosz, G., Wilson, R.E., Krauskopf, B.: Global bifurcation investigation of an optimal velocity traffic model with driver reaction time. Phys. Rev. E **70**, 026207 (2004)
40. Orosz, G., Stépán, G.: Subcritical Hopf bifurcations in a car-following model with reaction-time delay. Proc. R. Soc. A **462**, 2643-2670 (2006)
41. Sipahi, R., Niculescu, S.I.: Stability of car following with human memory effects and automatic headway compensation. Philos. Trans. Royal. Soc. A **368**, 4563-4583 (2010)
42. Kesting, A., Treiber, M.: How reaction time, update time, and adaptation time influence the stability of traffic flow. Comput. Aided Civil Infrastruct. Eng. **23**, 125-137 (2008)
43. Orosz, G., Moehlis, J., Bullo, F.: Robotic reactions: delay-induced patterns in autonomous vehicle systems. Phys. Rev. E **81**, 025204(R) (2010)
44. Ngoduy, D., Tampere, C.M.J.: Macroscopic effects of reaction time on traffic flow characteristics. Phys. Scr. **80**, 025802-025809 (2009)
45. Kang, Y.R., Sun, D.H.: Lattice hydrodynamic traffic flow model with explicit drivers' physical delay. Nonlinear Dyn. **71**, 531-537 (2013)
46. Ngoduy, D.: Analytical studies on the instabilities of heterogeneous intelligent traffic flow. Commun. Nonlinear Sci. Numer. Simul. **18**, 2699-2706 (2013)
47. Ngoduy, D.: Generalized macroscopic traffic model with time delay. Nonlinear Dyn. **77**, 289-296 (2014)
48. Chen, J.Z., Shi, Z.K., Yu, L., Peng, Z.Y.: Nonlinear analysis of a new extended lattice model with consideration of multi-anticipation and driver reaction delays. J. Comput. Nonlinear Dyn. **9**, 031005 (2014)
49. Davoodi, N., Soheili, A.R., Hashemi, S.M.: A macro-model for traffic flow with consideration of driver's reaction time and distance. Nonlinear Dyn. **82**, 1-8 (2015)

50. Xing, J.: A parameter identification of a car following model. In: Steps Forward. Intelligent Transport Systems World Congres, pp. 1739-1745 (1995)
51. Van Winsum, W.: The human element in car following models. Transp. Res. F **2**, 207-211 (1999)
52. Herman, R., Potts, R.B.: Single lane traffic theory and experiment. In: Proceedings of the Symposium on the Theory of Traffic Flow, pp. 120-146 (1961)
53. Chow, T.S.: Operational analysis of a traffic dynamics problem. Oper. Res. **6**, 165-184 (1958)
54. Liu, R., Li, X.: Stability analysis of a multi-phase car-following model. Physica A **392**, 2660-2671 (2013)
55. Wilson, R.E., Ward, J.A.: Car-following models: fifty years of linear stability analysis-a mathematical perspective. Transp. Planning Technol. **34**, 3-18 (2011)
56. Treiber, M., Kanagaraj, V.: Comparing numerical integration schemes for time-continuous car-following models. Physica A **419**, 183-195 (2015)

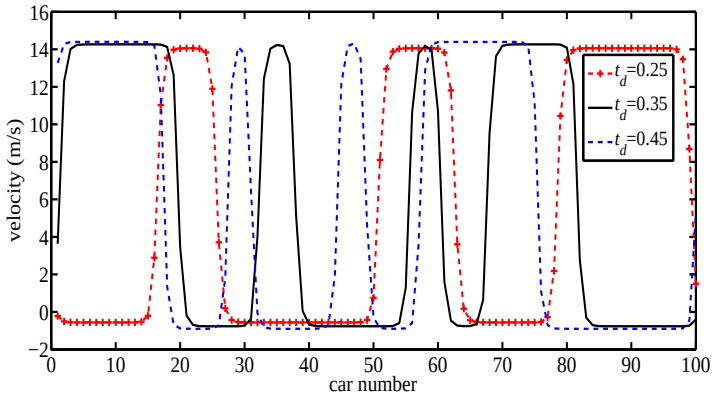

(a)

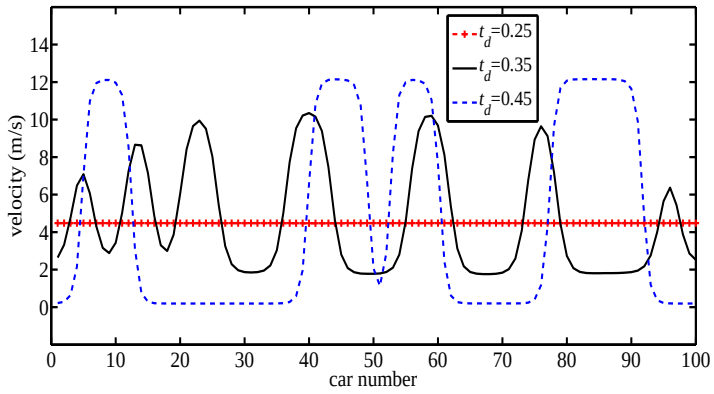

(b)

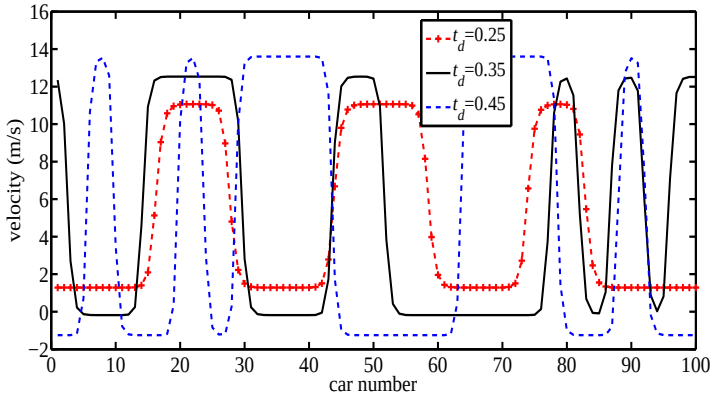

(c)

Fig. 9 Snapshot of velocities of all vehicles for different time delays. (a) $m = 3, \beta = 0$, (b) $m = 3, \beta = 0.5$, (c) $m = 1, \beta = 0.5$

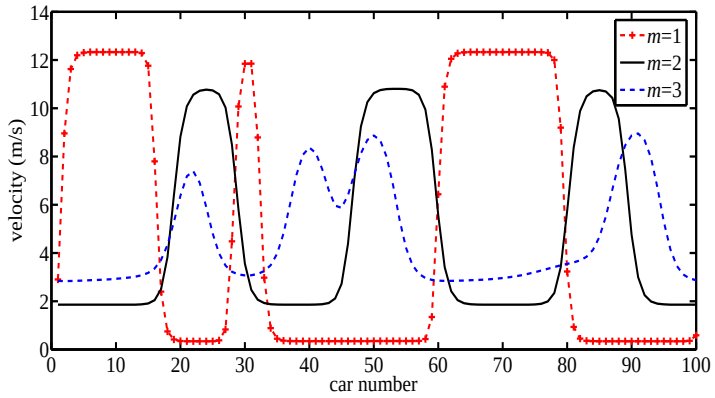

Fig. 10 Snapshot of velocities of all vehicles for different values of m

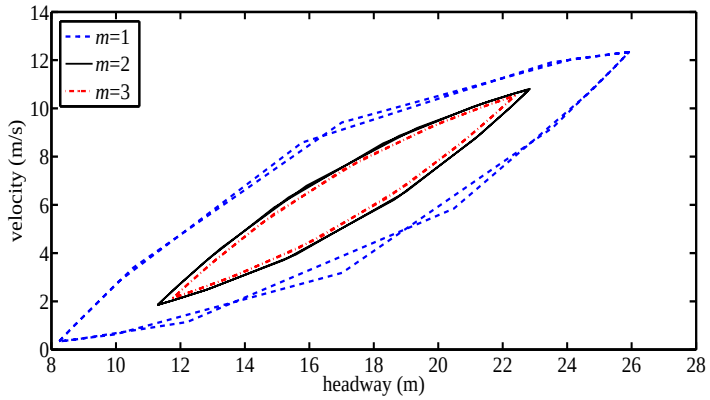

Fig. 11 The hysteresis loops for different values of m